THE ANATOMICAL RECORD 292:798–812 (2009)

The Relationship Between the Lizard Eye and Associated Bony Features: A Cautionary Note for Interpreting Fossil Activity Patterns

MARGARET I. HALL*
Department of Physiology, Arizona College of Osteopathic Medicine, Midwestern University, Glendale, Arizona

ABSTRACT

Activity pattern, the time of day when an animal is active, is associated with ecology. There are two major activity patterns: diurnal (awake during the day in a photopic environment) and nocturnal (awake at night in a scotopic environment). Lizards exhibit characteristic eye shapes associated with activity pattern, with scotopic-adapted lizard eyes optimized for visual sensitivity with large corneal diameters relative to their eye axial lengths, and photopic-adapted lizards optimized for visual acuity, with larger axial lengths of the eye relative to their corneal diameters. This study: (1) quantifies the relationship between the lizard eye and its associated bony anatomy (the orbit, sclerotic ring, and associated skull widths); (2) investigates how activity pattern is reflected in that bony anatomy; and (3) determines if it is possible to reliably interpret activity pattern for a lizard that does not have the soft tissue available for study, specifically, for a fossil. Knowledge of extinct lizards' activity patterns would be useful in making paleoecological interpretations. Here, 96 scotopic- and photopic-adapted lizard species are analyzed in a phylogenetic context. Although there is a close relationship between the lepidosaur eye and associated bony anatomy, based on these data activity pattern cannot be reliably interpreted for bony-only specimens, such as a fossil, possibly because of the limited ossification of the lepidosaur skull. Caution should be exercised when utilizing lizard bony anatomy to interpret light-level adaptation, either for a fossil lizard or as part of an extant phylogenetic bracket to interpret other extinct animals with sclerotic rings, such as dinosaurs. Anat Rec, 292:793–812, 2009.

Key words: vision; scotopic; photopic; sclerotic ring; orbit; lepidosaur

Activity pattern, the time of day when an animal is awake and active, is directly related to how much light is available for a visually dependent animal to create an image. There are two major activity patterns: diurnal, active during the day in a light-rich, or photopic, environment and nocturnal, active after sunset in a light-limited, or scotopic, environment. However, night is not the only light-limited environment. Many lizards are

Grant sponsors: Society of Integrative and Comparative Biology Grant-in-Aid-of-Research, the Field Museum of Natural History Visiting Scholarship, the Jurassic Foundation.

*Correspondence to: Margaret I. Hall, Department of Physiology, Arizona College of Osteopathic Medicine, Midwestern University, 19555 N 59th Ave, Glendale, AZ 85308. Fax: +623-572-3449. E-mail: margaretihall@yahoo.com

Received 30 October 2008; Accepted 30 December 2008
DOI 10.1002/ar.20889
Published online in Wiley InterScience (www.interscience.wiley.com).

diurnal, in that they are active during the day, but still utilize scotopic vision because they function in light-limited environments such as in burrows or under leaf litter. In woodland and forest environments, for example, it has been shown that multiple levels of shade produce light levels that are similar to those experienced by nocturnal animals (Endler, 1993). Previous studies have shown that the amount of light available to a visually dependent animal has a strong influence on the size and shape of that animal's eye: nocturnal lizards, and the nocturnal lepidosaur the tuatara, have a larger corneal diameter relative to the axial length of the eye (Ritland, 1982; Hall, 2008a), probably as an adaptation for increased visual sensitivity to light, whereas diurnal lizards exhibit a larger axial length of the eye relative to the corneal diameter, a shape correlated with increased visual acuity (Walls, 1942; Werner, 1969; Hughes, 1977; Martin, 1982, 1985, 1990; Ritland, 1982; Brooke et al., 1999; Ross, 2000; Land and Nilsson, 2002; Howland et al., 2004; Kirk, 2004, 2006; Hall, 2005, 2008a; Hall and Ross, 2007; Ross et al., 2007).

It is reasonable to expect eye size and shape to be correlated with the associated bony anatomy. Many bony structures are dependent on adjacent soft tissue to achieve normal adult shapes, including muscular and other soft tissues. Studies on bird development especially have shown that the sense organs, including the eye, exert a mechanical influence on normal skull morphogenesis (Hanken, 1983; Thorogood, 1988; Hanken and Thorogood, 1993): When eye formation is disrupted in embryonic chicks, orbit development is also disrupted (Columbre and Crelin, 1957; Tonneyckmuller, 1974; Vanlimborgh and Tonneyckmuller, 1976). For example, when microphthalmia (a pathologically small optic globe) occurs naturally or is artificially induced, the orbital structure conforms to the reduced size of the eye and general facial structure is malformed (Columbre and Crelin, 1957; Tonneyckmuller, 1974; Vanlimborgh and Tonneyckmuller, 1976). Similar observations have been made for infant humans (Taylor, 1939; Moss and Young, 1960).

The relationship between hard and soft tissue of the visual system has been most extensively studied in primates and avians. It has been shown that in small primates the eyeball fills a greater proportion of the orbit than in larger primates (Schultz, 1940). The relationships between activity pattern and bony anatomy of the orbit have also been investigated in both primates (Kay and Cartmill, 1977; Kay and Kirk, 2000; Kirk, 2006; Heesy and Ross, 2001) and avians (Hall, 2005, 2008b; Schmitz et al., 2007, Schmitz, 2008). For primates, as mammals, the bony correlate of eye size and shape is the morphology of the orbit itself. Kay and Cartmill (1977), in the context of an extant comparative base of similarly sized mammals, found that orbital aperture width relative to skull length separates nocturnal and diurnal primates with skull lengths less than 70 mm, and demonstrated that at small body sizes nocturnal primates exhibit larger orbit diameters than diurnal ones.

Information about both the corneal diameter and the axial length of the eye is necessary to interpret activity pattern. For primates, in the absence of the eye, it is possible to interpret corneal diameter from the orbit diameter. However, if no soft tissue is available, as for a fossil, it is only possible to infer the axial length of that portion of the eye that is directly contained within the orbit; there is no way to estimate how much of the eyeball protrudes from the bone. Additionally, because with increasing body size primate orbit volumes increase at a greater rate than eye volumes, at larger body sizes dimensions of the orbit do not accurately predict the size or shape of the eye (Schultz, 1940; Kay and Cartmill, 1977; Kay and Kirk, 2000; Heesy and Ross, 2001).

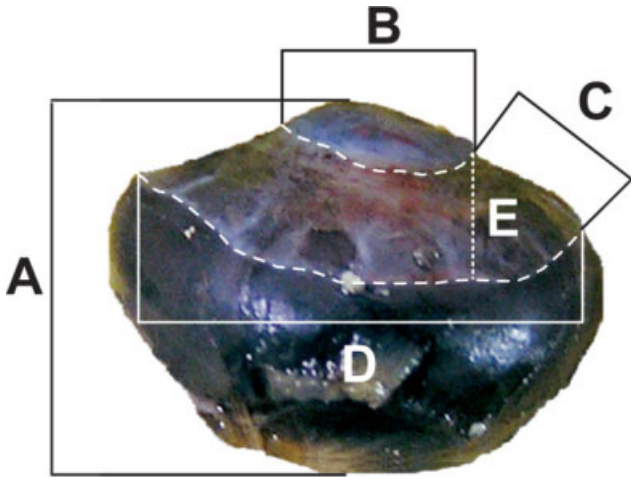

Fig. 1. Sclerotic ring and eye measurements, depicted on the eye of *Gecko gecko*. **A**: Axial length of the eye; **B**: inner diameter of the sclerotic ring and corneal diameter; **C**: maximum length of the sclerotic ring; **D**: outer diameter of the sclerotic ring; **E**: axial sclerotic ring length.

Lizards, however, like the great majority of diapsids, including birds, have an additional bony structure that is not present in mammals, the sclerotic ring. This structure houses that portion of the eyeball that extends from the orbit (Fig. 1). Because of the close association of the sclerotic ring with the soft tissue of the eye, it has been hypothesized that information about the soft tissue of the eye can be inferred from the dimensions of the sclerotic ring and that this information can be used for fossil interpretation in ichthyosaurs (Motani et al., 1999; Humphries and Ruxton, 2002; Fernandez et al, 2005), birds (Rowe, 2000; Hall 2004, 2005, 2008b; Schmitz et al., 2007, 2008), and dinosaurs (Hall, 2004; Rinehart et al., 2004; Hall et al., 2007; Schmitz et al., 2007, Schmitz, 2008). The extant distribution of sclerotic rings among terrestrial vertebrates is restricted to avians and lepidosaurs (Franz-Odendaal and Vickaryous, 2006), and both groups have been used as a comparative sample for fossil interpretations (Hall, 2004, 2005, 2008b; Rinehart et al., 2004; Schmitz et al., 2007, Schmitz 2008). However, to date, the nature of the relationship between the eye, orbit, and sclerotic ring has not been quantified for lizards.

The sclerotic ring may provide significantly more information about the dimensions of the optic globe than can the orbit alone (Franz-Odendaal and Hall, 2006; Franz-Odendaal and Vickaryous, 2006; Franz-Odendaal, 2008). The inner diameter of the sclerotic ring is virtually identical to the corneal diameter in lizards, and is therefore a much closer bony correlate than is orbit diameter. The outer edge of the sclerotic ring is associated with the orbital margin, and the ring houses a large

portion of the eye that protrudes from the orbit (Fig. 1; Romer, 1956; Proctor and Lynch, 1993). The sclerotic ring and orbit have been shown to vary their morphology according to light-level adaptation in avians (Hall, 2005, 2008b), and, like avians, lepidosaurs are highly visual and have large eyes relative to the size of their skulls or body size (Walls, 1942; Werner, 1969; Ritland, 1982; Werner and Seifan, 2006). Indeed, lepidosaur eyes are sufficiently large that they often meet at the midline or are separated by only a thin cartilaginous or fascial layer (Underwood, 1970). Currently, the evolution of activity pattern in lepidosaurs is not understood; if light-level adaptations were interpretable from hard-tissue characteristics alone, it might be possible to analyze the activity pattern for fossil lepidosaurs. Given the extant distribution of light-level adaptations, parsimony analysis indicates that the basal squamate may have been diurnal, but that the basal lepidosaur was of an unknown light-level adaptation (see Fig. 3).

Thus, this study has three aims: (1) to quantify the nature of the relationship between the eye, the sclerotic ring, and the associated skull in lizards, (2) to investigate how activity pattern is reflected in the bony anatomy that is associated with the eye, and (3) to determine if it is possible to reliably interpret activity pattern for lepidosaurs, such as fossils, that do not have soft tissue available for study.

MATERIALS AND METHODS

Study Animals

Data were collected on the eyeballs and related skull dimensions for 170 specimens of 96 lepidosaur species (Table 1). Study groups included both rhynchocephalians (tuatara) and squamates, including Iguanidae (iguanas), Agamidae (agamas), Chamaeoleonidae (chameleons), Geckonidae (geckos), Eublepharidae, Cordylidae (girdled lizards), Lacertidae (wall lizards), Xantusiidae (night lizards), Scincidae (skinks), Teiidae (whip-tailed lizards and tegus), Anguidae (alligator and glass lizards), and Helodermatidae (monitor lizards). Groups were chosen that included both nocturnal and diurnal animals. Specimens were obtained from the Department of Herpetology of the American Museum of Natural History (New York, NY), the Division of Amphibians and Reptiles of the Field Museum of Natural History (Chicago, IL), the Department of Zoology at the British National Natural History Museum (London, UK), and the California Academy of Sciences (San Francisco, CA). All of the specimens were preserved in ethanol, and individuals exhibiting any pathology or unusual preservational deformation were excluded from this study.

Measurements and Coding of Light Availability

Soft tissue. For alcohol-preserved specimens, to gain access to the eyeball, the eyelid was reflected or removed and the eye was removed from the orbit using closed, curved scissors and forceps to preserve the eye from accidental puncture. After removal from the orbit, the eyeball was cleaned of all extraocular muscles and remaining fascia, and was inflated using a small amount of preservative injected by a syringe inserted on an angle into the sclera just inferior to the outer edge of the sclerotic ring. Preservative was injected until the eye was fully inflated and would not accept any additional liquid. At that point, maximum corneal diameters and maximum axial lengths of the eye were measured to the 0.01 mm, either with digital calipers or with a reticle imbedded in a microscope eyepiece calibrated with digital calipers, depending on the size of the specimen (Fig. 1). For some lizards, membranes of various sizes and shapes protruded into the cornea from edge of the inner diameter of the sclerotic ring. The size of this membrane was not included in the measurement of the corneal diameter. Any eye that could not be fully inflated was not measured.

Hard tissue. All hard-tissue measurements were taken on wet specimens. The sclerotic ring cannot be separated from the eyeball and as such was measured on the eye after the soft-tissue measurements. As with the soft tissue, measurements were recorded to the 0.01 mm, either with digital calipers or with a reticle imbedded in a microscope eyepiece calibrated with digital calipers, depending on the size of the specimen. Two bony correlates of corneal diameter were measured: the maximum inner diameter of the sclerotic ring (Fig. 1) and orbital diameter. The maximum inner diameter of the sclerotic ring was the same measurement as the corneal diameter (Fig. 1). Orbital diameter was measured from orbitale inferius, defined as that point on the inferior orbital margin that is closest to the tooth row (Cartmill, 1970), to orbitale superius, defined as that point on the superior orbital margin that is opposite orbitale inferius (Cartmill, 1970). Four bony correlates of axial length of the eye were measured with digital calipers to 0.01 mm. The first two bony correlates of axial length are measurements of skull width that are highly associated with the orbital region (Fig. 2). The first width measurement was the distance from orbitale inferius to the midpoint of the skull roof (Fig. 2). The midpoint was usually easily identifiable because of a central scale. If there was no central scale present or it was difficult to locate the midpoint for some other reason, it was identified by measuring the distance between orbitale superius on the right and left orbits and then dividing that distance by two. The second width measurement was measured as the distance between the orbitale inferius on the right and left orbits, which was then halved and is called "one-half biorbitale inferius" in the discussion (Fig. 2). The second two correlates of axial length of the eye were on the sclerotic ring: sclerotic ring maximum length and a second measurement termed axial sclerotic ring length (ASRL), because it is that measure that is directly along the axial length of the eye (see Fig. 1). In lepidosaurs the maximum length of the sclerotic ring is obliquely oriented to the visual axis of the eye, and therefore may not accurately measure that portion of the axial length of the eye that is housed by the sclerotic ring. Therefore, the ASRL is an additional measurement of sclerotic ring length that is oriented along the axial length of the eye. ASRL was calculated by treating the maximum length of the sclerotic ring as the hypotenuse of a right triangle, and one-half the difference between the outer and inner diameters of the sclerotic ring as the base of the right triangle. The Pythagorean Theorem was then utilized to solve for the length of the remaining side of the right triangle (that portion parallel to the

TABLE 1. Species means raw data (all measurements in mm)

Taxon	N	Light level (ref[a])	AL	CD/sclerotic ring inner diameter	Orbit depth	Orbitale inferius-midline	Sclerotic ring max length	Axial sclerotic ring length	Orbit diameter	1/2 Biorbitale inferius	Head length	SVL
Anguidae												
Gerrhontus weighmanii	2	Photopic (1,9)	6.00	3.26	6.22	7.06	1.80	1.17	5.33	5.97	24.20	112.58
Chameleonidae												
Brookesia superciliaris	2	Photopic (4,5,9)	3.45	1.56	3.62	4.55	1.30	0.82	4.32	3.19	8.77	39.52
Chamaeleo africanus	2	Photopic (4,5,9)	7.73	2.26	9.81	10.85	2.54	2.07	9.68	7.89	28.51	131.62
Chamaeleo chamaeleon	2	Photopic (4,5,9)	7.39	2.23	7.49	9.88	2.73	2.17	9.31	6.56	24.21	70.66
Chamaeleo hoehnelli	2	Photopic (4,5,9)	5.58	2.34	6.96	9.50	1.41	1.11	7.78	6.10	24.85	84.66
Furcifer lateralis	2	Photopic (4,5,9)	6.72	1.81	6.34	8.62	1.93	2.28	7.79	5.43	20.50	76.15
Furcifer verrucosus	2	Photopic (4,5,99)	6.39	2.23	6.82	9.63	2.40	2.07	8.53	6.17	25.33	97.01
Cordylidae												
Chamaesaura macrolepis	1	Photopic (4,9)	2.93	1.73	3.59	4.07	1.60	1.60	3.29	–	15.43	125.88
Cordylus cordylus	3	Photopic (4,9)	4.85	3.00	6.50	7.24	1.64	1.06	5.40	–	24.62	86.82
Cordylus niger	3	Photopic (4,9)	4.19	2.21	6.45	7.03	1.69	1.20	5.33	5.84	22.50	72.45
Cordylus polyzonus	3	Photopic (4,9)	5.33	2.91	8.06	8.70	2.11	2.18	7.01	7.27	26.93	103.46
Platysaurus intermedius	2	Photopic (4,9)	3.78	2.27	3.18	5.85	1.37	1.28	4.57	5.01	19.32	81.06
Eublepharidae												
Eublepharus hardwickii	1	Scotopic (4,5,9)	6.71	6.31	7.00	–	3.16	3.16	8.10	–	–	100.21
Eublepharus macularis	1	Scotopic (4,5,9)	4.55	4.73	7.40	–	2.76	2.32	7.57	–	–	97.98
Geckonidae												
Coleonyx elegans	1	Scotopic (4,5,9)	4.62	4.51	4.55	–	2.62	2.60	5.80	–	–	82.96
Coleonyx variegatus	2	Scotopic (4,5,9)	2.59	0.85	4.19	4.47	1.52	1.41	4.13	–	12.02	60.40
Cyrodactylus louisiadensis	1	Scotopic (4,5,9)	11.59	9.35	10.58	–	2.99	2.97	9.46	–	34.45	137.32
Gekko gecko	1	Scotopic (4,5,9)	8.07	6.73	7.30	–	3.48	3.40	9.49	–	121.51	
Gehyra variegata	2	Scotopic (4,5,9)	3.33	3.01	3.48	4.13	1.97	1.95	3.89	–	11.42	42.31
Gekko swinhonis	2	Scotopic (4,5,9)	3.63	2.62	5.55	4.44	1.89	1.79	4.46	–	13.75	52.99
Gonatodes ocellatus	2	Photopic (7)	3.43	2.32	3.21	3.83	1.63	1.43	3.70	2.86	10.62	40.37
Gonatodes vittatus	2	Photopic (7)	2.83	1.80	2.70	3.38	1.12	0.99	3.42	2.67	8.53	32.65
Hemidactylus mabouia	2	Scotopic (9)	4.36	3.40	6.06	5.31	2.83	2.76	4.66	–	15.42	56.36
Hemidactylus platycephalus	2	Scotopic (9)	4.48	3.18	7.80	7.27	2.68	2.98	6.09	–	18.26	71.72
Lepidodactylus lugubris	2	Scotopic (9)	3.26	2.66	3.48	3.69	1.37	1.29	3.25	2.96	9.04	34.23
Lygodactylus picturatus	2	Photopic (7)	3.26	1.89	2.59	3.76	1.37	1.19	3.20	2.72	8.87	32.46
Narudasia festiva	1	Photopic (7)	2.23	1.72	2.64	2.96	1.03	1.00	2.44	2.33	8.59	28.69
Naultinus elegans	1	Scotopic (9)	5.02	3.02	4.73	–	2.48	2.37	–	–	–	68.50
Phyllodactylus reissii	1	Scotopic (9)	4.60	3.53.	7.93	–	2.02	1.91	5.34	–	17.15	64.20
Pristurus carteri	3	Photopic (7)	5.08	4.66	5.23	–	2.53	2.44	6.69	–	–	61.59
Ptyodactylus hasselquisti	1	Scotopic (9)	4.13	4.16	5.54	–	1.89	1.82	6.21	–	–	65.39
Quedenfeldtia moerens	2	Photopic (7)	4.03	2.49	4.54	4.58	1.63	1.36	3.93	3.57	11.73	43.41
Sphaerodactylus anthracinus	2	PhotopicPhotopic (7)	2.49	1.54	2.68	2.75	0.94	0.86	8.02	2.05	8.90	26.54
Tarentola mauritanica	1	Scotopic (9)	4.12	4.11	3.85	–	2.26	2.19	5.45	–	–	50.27
Phelsuma astriata	1	Photopic (7)	3.81	3.82	3.84	–	2.07	2.07	4.70	–	–	42.41
Phelsuma laticaudata	1	Photopic (7)	3.59	2.02	3.94	4.83	1.89	1.56	4.22	–	–	53.77
Phelsuma madagascariensis	1	Photopic (7)	4.22	3.02	6.76	8.42	1.70	1.20	6.35	–	–	81.78
Gerrhosauridae												
Gerrhosaurus major	2	Photopic (4,9)	6.01	3.53	8.33	10.19	3.13	2.00	8.64	8.17	28.00	128.38
Helodermatidae												
Heloderma[b]	1	Photopic (9)	8.23	4.29	10.92	–	4.29	3.06	9.10	19.14	57.68	313.04

TABLE 1. (*Continued*)

Taxon	N	Light level (ref[a])	AL	CD/sclerotic ring inner diameter	Orbit depth	Orbitale inferius-midline	Sclerotic ring max length	Axial sclerotic ring length	Orbit diameter	1/2 Biorbitale inferius	Head length	SVL
Iguanidae												
Amblyrynchus cristatus	2	Photopic (4,9)	7.04	4.27	11.23	15.62	2.89	1.88	10.57	10.93	31.23	148.15
Basiliscus vittatus	2	Photopic (4,9)	7.72	5.32	4.57	11.49	3.77	4.75	6.00	7.91	33.32	126.35
Callisaurus draconoides	2	Photopic (4,9)	4.39	2.99	5.84	6.42	1.73	1.25	5.67	–	14.33	64.88
Calotes mystaceus	2	Photopic (4,9)	9.51	2.15	6.92	10.15	1.97	–	8.20	7.26	22.99	80.71
Calotes versicolor	1	Photopic (4,9)	7.61	3.33	7.66	–	3.44	2.33	9.88	–	–	102.24
Crotaphytus bicinctores	2	Photopic (4,9)	3.32	1.39	—	–	–	–	–	–	21.25	81.40
Ctenosaura hemilopha	2	Photopic (4,9)	6.10	3.12	7.29	9.19	–	–	7.83	–	22.96	92.47
Ctenosaura similis	3	Photopic (4,9)	7.84	3.30	8.41	11.14	2.89	2.62	9.30	–	29.85	127.58
Dipsosaurus dorsalis	1	Photopic (4,9)	6.84	3.33	7.49	8.46	2.47	1.39	7.82	–	–	118.05
Draco melanopogon	2	Photopic (4,9)	5.74	2.78	3.24	6.07	1.88	1.00	5.79	4.70	12.68	81.47
Goniocephalus grandis	2	Photopic (4,9)	7.86	5.11	8.22	13.12	2.79	1.33	11.02	9.11	31.34	115.59
Iguana iguana	2	Photopic (4,9)	8.65	2.75	7.93	13.05	3.02	–	11.17	–	28.32	149.70
Leiocephalus carinatus	2	Photopic (4,9)	6.03	3.47	10.05	9.86	2.89	2.25	7.98	–	22.62	102.72
Leiolepis belliana	2	Photopic (4,9)	8.98	4.49	7.47	10.86	2.69	1.85	8.90	7.61	27.70	116.68
Physignathus longirostris	4	Photopic (4,9)	5.76	2.46	5.05	–	2.12	1.37	–	6.27	23.93	80.72
Sauromalus ater	2	Photopic (4,9)	7.88	4.05	9.26	11.96	–	–	9.17	–	30.80	150.55
Sceloporus grammicus	2	Photopic (4,9)	4.38	1.57	4.85	6.01	1.31	0.98	4.61	–	15.02	60.86
Sceloporus horridus	2	Photopic (4,9)	6.28	2.93	7.13	9.92	1.06	–	7.29	–	22.32	89.07
Sceloporus magister	2	Photopic (4,9)	7.18	3.00	11.29	10.9	2.81	1.43	8.88	–	28.13	114.43
Sceloporus oberon	2	Photopic (4,9)	5.37	2.62	6.21	8.60	1.81	0.94	6.54	–	21.10	83.18
Tropidurus hispidus	2	Photopic (4,9)	6.76	3.25	7.59	9.55	–	–	8.11	–	28.55	119.48
Uma exsul	2	Photopic (4,9)	5.05	2.43	6.61	7.49	2.49	1.97	6.37	–	15.72	83.13
Uranscodon superciliosus	2	Photopic (4,9)	8.79	4.86	10.74	14.33	3.82	1.83	12.02	–	34.96	129.34
Uromastix hardwickii	2	Photopic (4,9)	7.26	3.19	–	11.75	2.55	2.06	10.22	8.91	26.40	157.06
Uromaxtix microlepis	1	Photopic (4,9)	–	2.78	7.40	–	2.70		8.29	–	–	–
Lacertidae												
Acanthodactylus boskianus	3	Photopic (4,9)	3.33	1.46	3.37	5.02	1.67	1.19	4.55	4.06	14.06	59.37
Acanthodactylus cantoris	2	Photopic (4,9)	4.12	2.00	4.83	5.86	1.80	1.55	5.23	–	16.33	64.36
Acanthodactylus longipes	3	Photopic (4,9)	2.60	0.91	–	4.06	1.01	–	3.63	3.11	10.23	39.32
Acanthodactylus pardalis	2	Photopic (4,9)	2.85	1.09	3.58	4.93	6.16	5.71	4.75	4.00	13.85	61.59
Aporosaura anchietae	2	Photopic (4,9)	3.90	1.29	3.04	5.29	1.56	0.90	4.45	4.65	13.56	50.38
Eremias persica	1	Photopic (4,9)	4.06	2.11	3.13	7.11	2.03	1.35	5.26	–	–	87.83
Gallotia atlantica	2	Photopic (4,9)	3.51	1.64	3.73	6.52	1.60	1.06	4.46	5.39	19.65	76.14
Gallotia galloti	2	Photopic (4,9)	4.76	2.34	8.31	9.10	20.90	1.34	6.29	7.19	27.72	99.37
Gerrhosaurus nigrolineatus	1	Photopic (4,9)	5.07	2.50	5.80	8.28	1.56	–	6.76	6.48	22.25	105.15
Heliobolus lugubris	4	Photopic (4,9)	2.89	1.51	2.63	–	1.37	0.93	–	3.90	11.64	44.29
Ichnotropis squamulosa	3	Photopic (4,9)	3.90	1.59	–	5.57	1.74	0.86	5.03	4.55	16.63	70.59
Lacerta agilis	2	Photopic (4,9)	3.99	1.72	5.30	6.59	1.93	1.25	5.04	4.69	17.20	80.72
Lacerta viridis	3	Photopic (4,9)	4.69	2.58	5.49	7.95	2.34	1.87	6.48	6.02	23.59	98.00
Meroles knoxii	1	Photopic (4,9)	3.42	1.80	4.61	5.24	1.11	–	4.22	–	14.09	53.67
Mesalina guttulata	1	Photopic (4,9)	2.99	1.37	3.56	3.68	0.94	–	3.20	–	11.05	43.98
Ophisops sp.	1	Photopic (4,9)	2.94	1.76	2.53	4.74	1.01	0.62	4.10	–	11.17	43.94
Podarcis muralis	2	Photopic (4,9)	3.24	1.77	3.77	5.41	1.68	1.24	–	4.22	16.94	65.92
Takydromis septentrionalis	3	Photopic (4,9)	3.04	1.56	3.40	5.46	1.74	1.29	4.57	3.87	16.05	65.99
Scincidae												
Mabuya perrotetii	2	Photopic (2,6,10)	5.40	2.92	7.09	6.43	1.63	0.71	5.89	5.99	21.80	96.05
Scincus mitranus	1	Photopic (2,6)	5.15	2.40	4.64	6.99	1.72	1.03	4.59	5.07	18.70	98.63

TABLE 1. (*Continued*)

Taxon	N	Light level (ref[a])	AL	CD/sclerotic ring inner diameter	Orbit depth	Orbitale inferius-midline	Sclerotic ring max length	Axial sclerotic ring length	Orbit diameter	1/2 Biorbitale inferius	Head length	SVL
Tiliqua gigas	1	Photopic (2,6)	8.01	4.93	15.30	15.33	4.91	4.29	10.24	13.46	55.63	273.72
Egernia frerei	1	Scotopic (2,6,10)	6.44	4.93	9.58	13.21	4.09	3.52	9.40	9.32	35.41	180.93
Egernia whitei	1	Scotopic (10)	3.44	2.42	4.65	5.87	2.33	1.98	5.06	4.95	16.54	75.06
Eugongylus rufescens	1	Scotopic (2,6,10)	4.32	2.81	7.55	7.82	3.00	2.82	5.75	5.97	21.14	55.98
Sphenomorphus nigricaudis	1	Scotopic (2,6)	2.54	2.49	4.30	5.16	1.80	1.77	3.86	3.52	13.27	72.33
Teiidae												
Dracaena guianensis	1	Photopic (4,9)	12.01	6.86	13.77	17.52	5.15	3.83	13.51	14.32	62.63	178.63
Tupinambis nigropunctatus	2	Photopic (4,9)	9.00	5.32	7.94	10.91	3.52	2.50	9.70	7.79	31.69	120.17
Xantusiidae												
Lepidophyma gaigeae	2	Photopic (4,9)	2.69	1.89	3.27	3.97	0.88	0.61	3.22	3.22	12.94	56.57
Xantusia henshawi	2	Scotopic (3,9,11)	2.97	3.19	3.25	4.72	1.40	1.28	3.79	–	13.28	58.59
Xantusia riversiana	1	Scotopic (3,8,11)	4.91	3.55	5.00	6.69	2.55	2.45	4.94	–	21.13	81.54
Xantusia vigilis	2	Scotopic (3,8,11)	1.72	1.15	2.79	2.71	1.08	0.95	2.34	2.08	8.36	36.84
Rynchocephalia												
Sphenodon punctatus	1	Scotopic (9)	14.96	9.75	15.99	–	5.12	3.20	18.53	15.96	60.62	204.57

[a]Animals were coded for light availability from the literature (1 Smith, 1946; 2 Greer, 1989; 3 Fellers and Drost, 1991; 4 Cogger and Zwiefel, 1992; 5 Mattison, 1989; 6 Cogger, 1994; 7 Röll, 2001; 8 Pianka and Vitt, 2003; 9 Chapple, 2003) (10 Pianka, personal communication; 11 Herrel, personal communication).
[b]Helodermidae is cathemeral, or likely to be active at any time of day, and therefore potentially adapted to all light levels (Pianka and Vitt, 2003). Since there was only one cathemeral group in this study, it was not possible to consider this group independently statistically, so it was therefore categorized as photopic, based on earlier findings that cathemeral and crepuscular birds were not statistically different from diurnal birds (Hall, 2005; Hall and Ross, 2007).

Fig. 2. Skull width measurements that are hard-tissue correlates of axial length of the eye, depicted on a skull of *Agama agama*. Arrow **A**: Biorbitale inferius, defined as the distance between orbitale inferius on the right and left orbits. Orbitale inferius is defined as that point on the inferior orbital margin that is closest to the tooth row (Cartmill, 1970). All statistical analyses performed with this measurement utilized one-half this distance and is called one-half biorbitale inferius. Arrow **B**: Orbitale inferius to the midline of the skull roof.

optic axis), and the result used as the ASRL (Fig. 1). Head length was measured from the tip of the snout to the opening of the external auditory meatus. Not every measurement was available for every specimen (see Table 1).

All the lizards were coded for activity pattern from the literature (Table 1). This study includes several animals that are diurnal, in that they are active during the day, but still utilize scotopic vision because they function in light-limited environments such as burrows, rock crevices, or under leaf litter. Therefore, all the lizards in this study were coded as scotopic or photopic rather than as nocturnal or diurnal.

Data Analysis

Standard statistical analysis: Comparisons between soft and hard tissue. To quantify the relationship between soft and hard tissue in the lepidosaur visual system, regressions were calculated between two soft tissue measurements of the eye, axial length and corneal diameter, and relevant hard tissue variables. Measurement error and natural variation affect both dependent and independent variables; therefore, reduced major axis (RMA) was the Model-II line-fitting technique utilized in this study; this method does not assume that variance in either variable is more significant (Ricker, 1984; Rayner, 1985; Plotnick, 1989; Sokal and Rohlf, 1995). To determine the nature of the relationship between the axial length of the eye and its hard-tissue correlates, RMA regressions were calculated with four different bony measurements, including: (1) the maximum length of the sclerotic ring, (2) the ASRL, (3) orbitale inferius to the midline of the skull, and (4) one-half biorbitale inferius. Corneal diameter has a close relationship with two bony measurements, the inner diameter of the sclerotic ring and orbit diameter. Because all measurements were taken on wet specimens, the eye and sclerotic ring are not separate. As such, the

measurements of the corneal diameter and the inner diameter of the sclerotic ring were identical, so no statistics were necessary to compare the two. However, orbit diameter, a useful variable in determining light-level adaptation in primates, was regressed against corneal diameter.

Standard statistical analysis: Activity pattern analysis utilizing hard-tissue-only measurements. Previous work has shown that analyses of the soft-tissue variables corneal diameter and axial length of the eye reliably separates scotopic-adapted from photopic-adapted lizards (Hall, 2008a). Therefore, the relevant hard-tissue variables were here analyzed, and both regression and ANOVA analyses were performed to determine if hard-tissue characteristics alone can separate scotopic and photopic lizards.

Previous work has shown that head length is an important variable in interpreting light-level adaptation in bony-only primate specimens (Kay and Cartmill, 1977; Kay and Kirk, 2000; Heesy and Ross, 2001). The hard-tissue variables identified in this study as being closely related to axial length of the eye are also expected to be related to head length, including sclerotic ring length, the distance between orbitale inferius and the midline, and one-half biorbitale inferius, and therefore these relationships were here investigated.

The inner diameter of the sclerotic ring, a close bony correlate of corneal diameter, was regressed against head length and the four bony correlates of the axial length of the eye (sclerotic ring length, ASRL, orbitale inferius to the midline, and one-half biorbitale inferius). In primates, the nature of the relationship between orbit diameter and head length has been shown to be useful for interpreting activity pattern (Kay and Cartmill, 1977). For mammals, orbit diameter is the only bony correlate of corneal diameter, but in lepidosaurs, the inner diameter of the sclerotic ring is the same measurement as the corneal diameter, and as such this measurement may be more useful than orbit diameter in interpreting lepidosaur activity pattern, so both variables are analyzed. Also, the relationships between orbit diameter and two bony variables related to axial length of the eye are analyzed, including the distance between orbitale inferius and the midline and one-half biorbitale inferius.

Initially, a single RMA line was calculated for each regression, and residuals were calculated from that line for all lepidosaurs plotted. The residuals were not normally distributed, so a Kruskal–Wallis nonparametric alternative to ANOVA was calculated comparing scotopic and photopic lizards. Then, for each pair of variables, two RMA lines were calculated; one for scotopic lizards and the other for photopic lizards. The regression lines were then tested for homogeneity, and then analysis of covariance (ANCOVA) was used to interpret the differences in elevation for scotopic and photopic lizards (Sokal and Rohlf, 1995). Both techniques were utilized to confirm the ANCOVA results for differences between groups and to compare the differences between scotopic and photopic animals in situations where the individual scotopic and photopic RMA slopes were not homogeneous and therefore not appropriate for ANCOVA analysis.

Fossils are often incomplete specimens, and it would be useful if there were single hard-tissue variables that showed consistent differences between scotopic and photopic lizards. To investigate this, six one-way ANOVAs were calculated to determine if there was a significant difference between the groups for single hard-tissue variables, including (1) $\log_{10}$ inner diameter of the sclerotic ring, (2) $\log_{10}$ orbit diameter, (3) $\log_{10}$ maximum sclerotic ring length, (4) $\log_{10}$ orbitale inferius to the midline, (5) $\log_{10}$ one-half biorbitale inferius, and (6) the $\log_{10}$ shape ratio of the inner diameter of the sclerotic ring (the bony correlate of corneal diameter): orbitale inferius to the midline (a bony correlate of the axial length of the eye). The shape ratio allows for an examination of the shape of the sclerotic ring and associated without the influence of size. To ensure that the ratio has no remaining relationship with size, the ratio was regressed against head length.

Finally, discriminant function analysis was run on all the logged hard-tissue variables that were shown to statistically discriminate between scotopic and photopic lizards based on Kruskal–Wallis analyses of the residuals from the RMA slopes (as described earlier) (Hair et al., 1998). These variables are: inner diameter of the sclerotic ring, one-half biorbitale inferius, orbitale inferius to the midline of the skull, snout-vent length, head length, and sclerotic ring length. All variables were entered into the discriminate matrix simultaneously. Group membership was computed from group sizes (which were unequal) based on the within-group covariance matrix values.

Phylogenetic comparative methods. Conventional statistical methods assume that data observations are independent (e.g., Sokal and Rohlf, 1995). However, data observations in closely related animals may violate the assumption of independence, requiring specialized statistical methods (Felsenstein, 1985). Here, independent contrast analysis (Felsenstein, 1985; Harvey and Pagel, 1991) is used to analyze the relationships between soft-tissue variables and their hard-tissue correlates, and also between hard-tissue variables and activity pattern in a phylogenetic context. At the present time, there is no single phylogeny that includes all the animals in this study. Therefore, the tree utilized in this study is a composite of individual lower taxonomic level molecular phylogenies as follows: Chamaeleonidae (Townsend and Larson, 2002), Iguanians (Schulte et al., 1998, 2003; Wiens and Hollingsworth, 2000; Frost et al., 2001), Gekkotans (Donnellan et al., 1999; Carranza et al., 2002; Han et al., 2004), Cordylidae (Frost et al., 2001; Odierna et al., 2001; Whiting et al., 2003), Xantusiidae (Vicario et al., 2002, Whiting et al., 2003), Scincidae (Whiting et al., 2003), Lacertidae (Fu, 1997; Whiting et al., 2003); Teiidae (Fitzgerald, et al., 1999; Reeder et al. 2002; Whiting et al., 2003), Anguidae (Macey et al., 1999), and Varanoidea (Lee, 1998; Macey et al., 1999). These individual composite lower level group phylogenies were then assembled into a large-scale composite phylogeny in Mesquite (Maddison and Maddison, 2003) that reflects interordinal relationships from Lee et al. (2004) and the composite phylogeny in Metzger and Herrel (2005) (see Fig. 3). Of the total of 96 species included in the standard statistical analysis, it was possible to construct a phylogeny that included 70 taxa. Whenever possible, more resolved trees were always chosen. Branch lengths were set as equal.

This study combines continuous (measurements of eye size and shape) and discrete (activity pattern) variables.

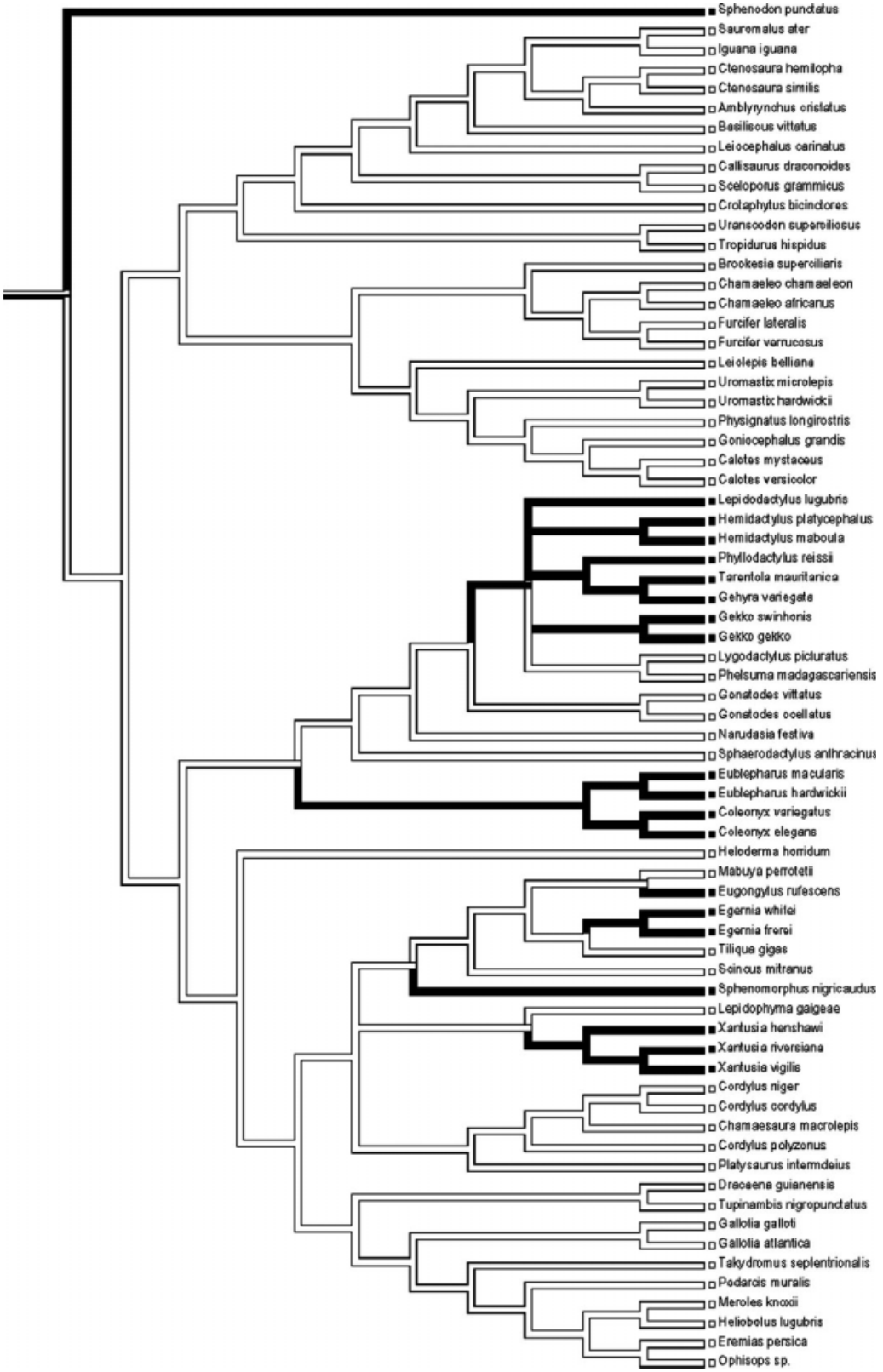

Fig. 3. Composite phylogeny of lepidosaurs used to calculate phylogenetic independent contrasts. The extant distribution of light levels is known (see Table 1), and the probable ancestral light levels are determined by the most parsimonius distribution (Mesquite 1.05, Maddison and Maddison, 2003), which indicates that the basal squamate was probably diurnal and the basal lepidosaur was of an unknown activity pattern.

TABLE 2. Summary results for RMA regression analyses (all variables are log_{10})

Light-level adaptation	*Y*-variable	*X*-variable	RMA slope	CI	r^2	OLS slope	PIC OLS slope	Significant ANCOVA?
Photopic	Sclerotic ring length	Head length	1.141	0.942–1.382	0.462	0.776		
Scotopic	Sclerotic ring length	Head length	0.898	0.684–1.18	0.749	0.777		
Both	Sclerotic ring length	Head length	1.08	0.92–1.27	0.498	0.76	0.9543	not homog.
Photopic	Orbitale inferius-midline	Head length	0.988	0.905–1.08	0.886	0.93		
Scotopic	Orbitale inferius-midline	Head length	1.042	0.904–1.2	0.949	1.015		
Both	Orbitale inferius-midline	Head length	1.01	0.94–1.08	0.901	0.956	0.8462	no
Photopic	1/2 Biorbitale inferius	Head length	0.951	0.881–1.027	0.939	0.93		
Scotopic	1/2 Biorbitale inferius	Head length	0.983	0.856–1.13	0.981	1.015		
Both	1/2 Biorbitale inferius	Head length	0.96	0.9–1.024	0.949	0.956	0.8817	no
Photopic	Sclerotic ring inner diameter	Head length	0.927	0.791–1.086	0.614	0.726		
Scotopic	Sclerotic ring inner diameter	Head length	1.213	0.824–1.787	0.723	1.032		
Both	Sclerotic ring inner diameter	Head length	1	0.87–1.16	0.602	0.779	0.732	not homog.
Photopic	Sclerotic ring inner diameter	Ring max length	0.818	0.662–1.01	0.27	0.426		
Scotopic	Sclerotic ring inner diameter	Ring max length	1.39	1.001–1.928	0.6	1.082		
Both	Sclerotic ring inner diameter	Ring max length	0.983	0.821–1.77	0.321	0.557	0.5022	not homog.
Photopic	Sclerotic ring inner diameter	ASRL	0.908	0.716–1.15	0.107	0.39		
Scotopic	Sclerotic ring inner diameter	ASRL	1.348	1.04–1.75	0.608	0.996		
Both	Sclerotic ring inner diameter	ASRL	1.01	0.84–1.2	0.299	0.551		not homog.
Photopic	Sclerotic ring inner diameter	Orb. inf.-ml.	0.965	0.826–1.128	0.634	0.769		
Scotopic	Sclerotic ring inner diameter	Orb. inf.-ml.	1.153	0.632–2.102	0.491	0.808		
Both	Sclerotic ring inner diameter	Orb. inf.-ml.	0.96	0.825–1.118	0.596	0.741	0.8298	yes
Photopic	Sclerotic ring inner diameter	1/2 biorb. inf.	0.816	0.675–0.987	0.652	0.736		
Scotopic	Sclerotic ring inner diameter	1/2 biorb. inf.	1.005	0.911–1.09 0.99	0.908			
Both	Sclerotic ring inner diameter	1/2 biorb. inf.	0.957	0.804–1.139 0.629	0.759		0.8042	not homog.
Photopic	Orbit diameter	Head length	0.845	0.737–0.959	0.724	0.696		
Scotopic	Orbit diameter	Head length	0.953	0.852–1.246	0.822	0.927		
Both	Orbit diameter	Head length	0.833	0.787–0.991	0.749	0.764	0.667	not homog.
Photopic	Orbit diameter	Orb. inf.-ml	0.894	0.797–1.003	0.798	0.798		
Scotopic	Orbit diameter	Orb. inf.-ml	0.859	0.738–0.996	0.943	0.832		
Both	Orbit diameter	Orb. inf.-ml	0.908	0.82–0.98	0.833	0.822	0.7458	no
Photopic	Orbit diameter	1/2 biorb. inf.	0.816	0.675–0.987	0.652	0.659		
Scotopic	Orbit diameter	1/2 biorb. inf.	1.005	0.911–1.09	0.99	1		
Both	Orbit diameter	1/2 biorb. inf.	0.871	0.75–1.012	0.737	0.748	0.7049	not homog

ASRL, axial sclerotic ring length; Orb. inf.-ml, orbitale inferius to the midline; 1/2 biorb. inf, One-half biorbitale inferius.

TABLE 3. Summary results for comparisons between hard and soft tissue

Soft-tissue variable	Hard-tissue variable	r^2	RMA slope	CI	OLS slope	PIC OLS slope
Axial length of the eye	Sclerotic ring max length	0.277	0.795	0.669–0.945	0.715	0.703
Axial length of the eye	Axial sclerotic ring length	0.244	0.926	0.77–1.114	0.458	
Axial length of the eye	Orbitale inferius-midline	0.859	0.93	0.854–1.01	0.86	0.855
Axial length of the eye	1/2 Biorbitale inferius	0.801	0.922	0.812–1.05	0.839	0.834
Corneal diameter	Orbit diameter	0.276	0.967	0.813–1.15	0.839	0.7561

TABLE 4. Summary results of residual analyses between light-level adaptations

Y-variable	*X*-variable	RMA regression equation	Kruskal-Wallis Asymp. Sig.	χ^2
Sclerotic ring inner diameter	1/2 Biorbitale inferius	$y = (0.957)(x) - 0.310$	0.012	6.312
Sclerotic ring inner diameter	Orbitale inferius-midline	$y = (0.96)(x) - 0.426$	0.024	5.126
Sclerotic ring inner diameter	Head length	$y = (1)(x) - 0.9$	0.006	7.439
Sclerotic ring inner diameter	Sclerotic ring length	$y = (0.983)(x) + 0.108$	0.004	8.095
Orbit diameter	1/2 Biorbitale inferius	$y = (0.871)(x) + 0.132$	0.33	0.948
Orbit diameter	Orbitale inferius-midline	$y = (0.908)(x) + 0.007$	0.322	0.948
Orbit diameter	Head length	$y = (0.833)(x) - 0.991$	0.099	2.729

Phylogenetic independent contrasts for this study were performed in CAIC (v2.6.9) (Purvis and Rambaut, 1995) because this program does not require a fully resolved tree and it is able to analyze a combination of continuous and discrete variables utilizing the BRUNCH algorithm (Purvis and Rambaut, 1995; Nunn and Barton, 2001). The null hypothesis tested by BRUNCH is that the dependent continuous variables (the morphological measurements) are not related to the independent discrete variable (activity pattern). BRUNCH calculates contrasts only at those nodes where the discrete variable changes, in this case, where there is a transition between photopic and scotopic activity patterns (Purvis and Rambaut, 1995). The sign of the contrast depends of the direction of the discrete variable change; if zero, there is no change and the null hypothesis of no relationship between the morphological and discrete variables is not rejected. Individual BRUNCH analyses were run for all six of the continuous morphological variables (sclerotic ring inner diameter, orbit diameter, sclerotic ring length, orbitale inferius to the midline, one-half biorbitale inferius, and the shape ratio sclerotic ring inner diameter: orbitale inferius to the midline).

RESULTS

Allometry of the vertebrate eye is generally observed to scale with negative allometry to body size (Ritland, 1982; Kiltie, 2000; Werner and Seifan, 2006; Hall, 2005, 2008a; Hall and Ross, 2007; Ross et al., 2007). However, in this study, the bony correlates of axial length of the eye (sclerotic ring length, orbitale inferius to the midline, and one-half biorbitale inferius) scale nearly isometrically with head length (Table 2). One bony correlate of corneal diameter, sclerotic ring inner diameter, also scales isometrically with head length (see Table 2). Orbit diameter, another bony correlate of corneal diameter, is the only variable to scale with negative allometry against head length (see Table 2).

Comparisons Between Soft and Hard Tissue

All correlations between soft-tissue variables and their hard-tissue correlates were significant ($P < 0.001$) (Table 3). However, for some of these correlations, very little of the variance observed is explained, as shown by low r^2 results. Axial length of the eye versus maximum sclerotic ring length has an r^2 value of only 0.27 and axial length of the eye versus ASRL has an r^2 of only 0.244; the relationships of the axial length of the eye with orbitale inferius to the midline ($r^2 = 0.859$) and with one-half biorbitale inferius ($r^2 = 0.801$) are stronger. The corneal diameter also has a comparatively weak relationship with the orbit diameter ($r^2 = 0.276$), but is identical to the inner diameter of the sclerotic ring.

Activity Pattern Analysis Utilizing Hard-Tissue-Only Measurements

As discussed in the Materials and Methods section, the residuals calculated from the RMA regression lines were not normally distributed, so a Kruskal–Wallis nonparametric alternative to ANOVA was performed to determine whether there was a difference between the scotopic and photopic groups (Table 4). All of these Kruskal–Wallis tests for residuals from lines with the inner diameter of the sclerotic ring as the *y*-variable were significant, and those using orbit diameter as the *y*-variable were not significant.

RMA lines were then calculated individually for scotopic and photopic lizards for each pair of hard-tissue variables. For every regression where the slopes were homogeneous, ANCOVA results showed nonsignificant differences in elevation between groups except for $\log_{10}$ sclerotic ring inner diameter on the *y*-axis and $\log_{10}$ orbitale inferius to the midline on the *x*-axis, where the ANCOVA results showed significant differences in elevation between groups (Fig. 4 and Table 2). Because all additional scatter plots are similar and generally not significant, only one additional scatter plot is displayed as an example, $\log_{10}$ sclerotic ring inner diameter on the *y*-axis and $\log_{10}$ head length on the *x*-axis (Fig. 5).

All one-way ANOVAs performed on logged single hard-tissue variables were nonsignificant except for the inner diameter of the sclerotic ring, orbitale inferius to the midline, and the shape ratio sclerotic ring inner

diameter/orbitale inferius to the midline (Table 5). Sclerotic ring length was not normally distributed, so a Kruskal–Wallis test was performed that also showed no significant difference between groups.

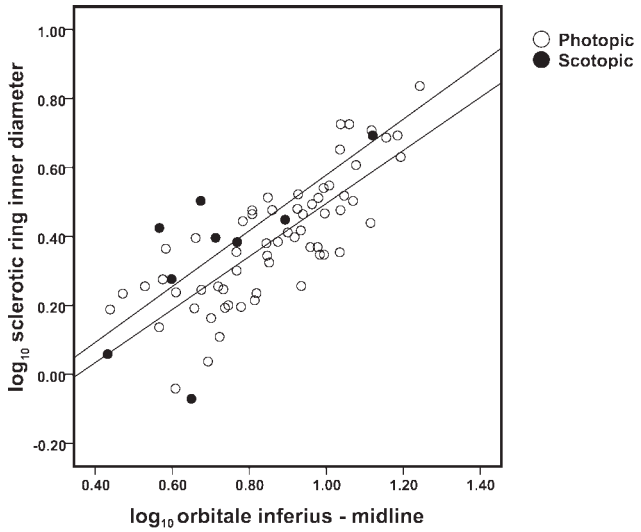

Fig. 4. Scatter plot of $\log_{10}$ sclerotic ring inner diameter (a bony correlate of corneal diameter) and $\log_{10}$ orbitale inferius to the midline (a bony correlate of axial length of the eye).

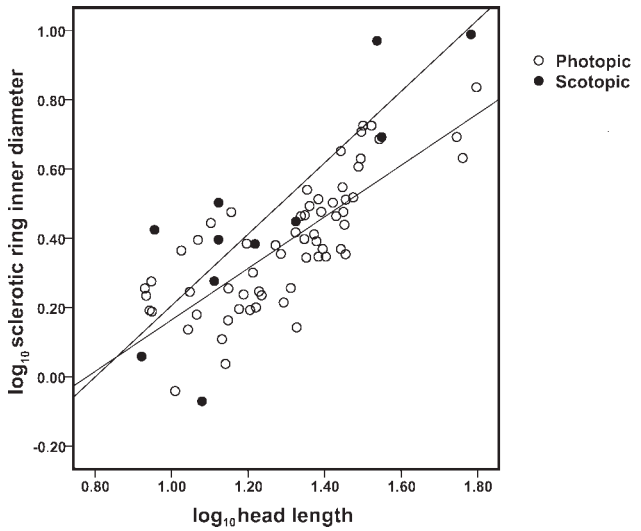

Fig. 5. Scatter plot of $\log_{10}$ sclerotic ring inner diameter (a bony correlate of corneal diameter) and $\log_{10}$ head length.

There was very little variance explained in the relationship between the shape ratio and head length, suggesting that this ratio can be used to examine shape differences between scotopic and photopic lizards with little relationship with size ($r^2 = 0.11$).

The BRUNCH algorithm of CAIC calculated phylogenetic independent contrasts at six nodes where there was a change between activity patterns. All BRUNCH analyses revealed nonsignificant differences between scotopic and photopic lizards.

Discriminant function analysis was run on all the logged hard-tissue variables where Kruskal–Wallis analyses of the residuals from the RMA slopes statistically separated scotopic and photopic lizards (inner diameter of the sclerotic ring, half of biorbitale inferius, orbitale inferius to the midline of the skull, snout-vent length, head length, and sclerotic ring length). Because only two states were analyzed (scotopic and photopic), only a single canonical discriminant function was produced; based on the computed Wilks-Lambda value (0.854, df = 6) this result was not significant ($P = 0.358$). Therefore, animals also cannot be distinguished into light-availability groups on the basis of the multivariate variance in these data.

DISCUSSION

Comparisons Between Soft and Hard Tissue

There is a strong relationship between many soft-tissue variables and their hard-tissue correlates. The corneal diameter and inner diameter of the sclerotic ring are literally the same measurement, and axial length of the eye is well correlated with both the distance between orbitale inferius to the midline ($r^2 = 0.859$) and one-half biorbitale inferius ($r^2 = 0.801$). The RMA slopes between axial length of the eye and both orbitale inferius to the midline and one-half biorbitale inferius indicate relationships that are nearly isometric, with 1 included in the confidence intervals. Orbit diameter and corneal diameter, however, have a weaker relationship, with an r^2 of only 0.276, as does axial length of the eye with maximum sclerotic ring length, ($r^2 = 0.277$) and with ASRL ($r^2 = 0.244$).

Activity Pattern Analysis Utilizing Hard-Tissue Only Measurements

Soft-tissue-only analysis has shown that the shape of a lizard's eyeball reflects its light-level adaptation: Scotopic lizards have a larger corneal diameter relative to the axial length of the eye, and photopic lizards have a longer axial length of the eye relative to the corneal diameter (Hall, 2005, 2008a). The purpose of this study is to investigate the use of bony variables, including single

TABLE 5. Results for comparisons between means (all variables are $\log_{10}$)

Variable	Significance	Statistic	Statistic
Inner diameter sclerotic ring	$P = 0.016$	F-value = 6.941	ANOVA
Orbit diameter	$P = 0.181$	F-value = 1.815	ANOVA
1/2 Biorbitale inferius	$P = 0.490$	F-value = 0.484	ANOVA
Sclerotic ring length	asymp. sig.=0.194	$\chi^2 = 1.686$	Kruskal-Wallis
Orbitale inferius-midline	$P = 0.01$	F-value = 7.041	ANOVA
Sclerotic ring inner diameter/orbitale inferius to the midline	$P = 0.02$	F-value = 5.707	ANOVA

bony variables, to determine light-level adaptation in a bony-only specimen that is not complete, specifically, for a fossil. Scotopic lizards exhibit a larger sclerotic ring inner diameter, the bony correlate of corneal diameter, relative to a smaller distance from orbitale inferius to the midline, the bony correlate of axial length. Photopic lizards exhibit the opposite pattern, with a smaller sclerotic ring inner diameter relative to a larger distance from orbitale inferius to the midline (see Table 5 and Fig. 6). Regression analysis of these two variables, with sclerotic ring inner diameter on the *y*-axis and orbitale inferius to the midline on the *x*-axis (Table 2 and Fig. 4), shows the only significant ANCOVA analyses of elevational differences between RMA slopes of scotopic and photopic lizards; all other variables are either not homogenous and therefore not appropriate for ANCOVA analyses, or are not significantly different. Likewise, the sclerotic ring inner diameter, the distance between orbitale inferius to the midline, and the shape ratio between the two variables are the only single variables with significant differences between the means of scotopic and photopic lizards (Fig. 6). However, in all cases, there is significant overlap in the distributions of scotopic and photopic lizards, and it would be difficult to analyze any individual lizard for light-level adaptation without associated soft tissue, such as for a fossil. As seen in Table 5 and Fig. 6, virtually every scotopic specimen included in this study is within the photopic range, so although it might be possible to exclude the possibility of scotopic adaptation for a skeletal-only specimen, it would be difficult to support a conclusion of a scotopic adaptation. Additionally, the sclerotic ring must be present for interpretations of light-level adaptations; this study shows that all analyses utilizing the orbit diameter as the bony correlate for corneal diameter, a variable highly useful for discriminating between light-level adaptations for primates (Kay and Cartmill, 1977; Kay and Kirk, 2000; Heesy and Ross, 2001, 2004; Ross et al., 2007), show no significant differences between scotopic and photopic lizards (Fig. 5).

Analysis of phylogenetic independent contrasts did not show significant differences between scotopic and photopic lizards for any of the variables. PIC analysis of the associated soft-tissue variables yielded significant results for the shape ratio of corneal diameter/axial length of the eye. Here the shape ratio using hard-tissue correlates, like all the size variables, was not found to be significant in a phylogenetic context. This may because the sample size was smaller (70 lepidosaurs total vs. 96 in the soft-tissue sample size, and all measurements were only available for nine scotopic lizards in the hard-tissue analysis vs. 18 for the soft-tissue analysis) (Hall, 2008a). Also, only six contrasts were calculated by the BRUNCH

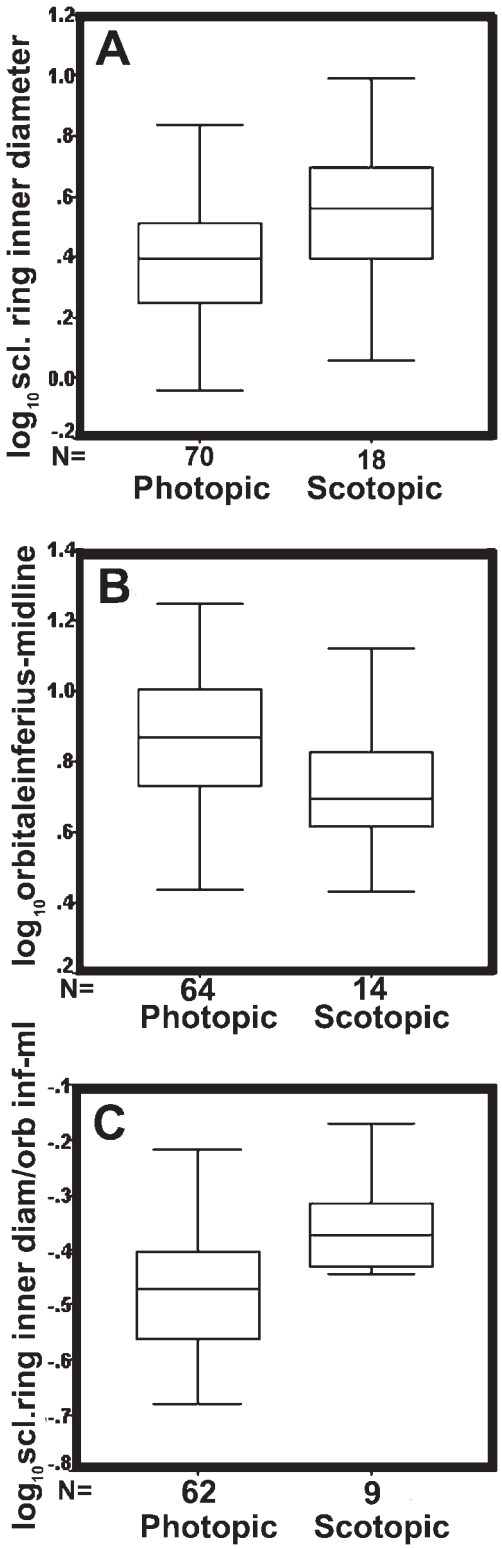

Fig. 6. Three box-and-whiskers plots; in all cases, the solid line within the box represents the median, the length of the box represents the interquartile range, and the whiskers represent the largest and smallest variables that are not outliers (Green et al., 2000). (**A**) Box-and-whiskers plot of $\log_{10}$ inner diameter of the sclerotic ring, showing the differences between photopic and scotopic lepidosaurs. ANOVA analysis found the differences between the means to be statistically significant ($P = 0.016$). (**B**) Box-and-whiskers plot of $\log_{10}$ orbitale inferius to the midline, showing the differences between photopic and scotopic lepidosaurs. ANOVA analysis found the differences between the means to be statistically significant ($P = 0.01$). (**C**) Box-and-whiskers plot of $\log_{10}$ shape ratio sclerotic ring inner diameter/orbitale inferius to the midline, showing the differences between photopic and scotopic lepidosaurs. ANOVA analysis found the differences between the means to be statistically significant ($P = 0.02$).

algorithm of CAIC versus seven for the soft-tissue sample. A PIC analysis of the shape ratio may be significant for an increased hard-tissue sample size.

Because of the fragile nature of most extant lizard sclerotic rings, and the fact that no fossil lepidosaur sclerotic rings have been discovered to date (S. Evans, personal communication), it may be unlikely that a fossil sclerotic ring will ever be available for analysis. It may be that the measurement of orbitale inferius to the midline might be preserved in a fossil lepidosaur, even if that specimen was flattened. However, as seen in Fig. 6c, although there is a statistically significant difference between the means of this measurement between the two groups, the overlap is so large that just this information will not allow for interpretation of an individual lizard's light-level adaptation, except in the extreme of the photopic range. However, it is interesting to note that although this hard-tissue variable is different between scotopic and photopic lizards, the associated soft-tissue characteristic, axial length of the eye, is not significantly different between the groups, and differences in eye shape are affected by changes in corneal diameter alone (Hall, 2005, 2008a). Head width measurements are not only correlates of eye size and shape but are also part of other complexes of traits in the head, such as brain size and bite force. Avians (Proctor and Lynch, 1993; Hall, 2005, 2008b) and primates (Kay and Kirk, 2000; Heesy and Ross, 2001; Kirk, 2006), the animals for which bony anatomy of the visual system has been successfully analyzed for light-level interpretations, both have ossified orbit depths, the distance from the orbital margin to the optic foramen. In avians the measurement of orbital depth together with the length of the sclerotic ring (Hall, 2005, 2008b) is closely correlated with the axial length of the eye. As such, orbital depth plus sclerotic ring length is central to interpreting activity pattern for avian skeletal specimens lacking the associated eyeball (Hall, 2005, 2008b). However, the structure of the orbit and sclerotic ring varies considerably across diapsids. In many lepidosaurs, the entry of the optic nerve into the orbit is a soft-tissue structure, and an orbit depth comparable to that of avians and many mammals is unavailable. However, although the axial length of the eye is well correlated with adjacent skull widths, these skull width measurements do not differentiate between activity patterns: axial length of the eye is not different between scotopic and photopic lepidosaurs (Hall, 2005, 2008a), but, as discussed earlier, the two measurements of skull width utilized in this study are different in the two groups. Therefore, in lepidosaurs, the nature of the relationship between soft and hard tissue associated with the visual system is such that hard-tissue characteristics alone are not sufficient to interpret light-level adaptation, such as for a fossil lepidosaur.

The data presented here indicate that caution should be exercised when utilizing lepidosaur sclerotic rings to interpret light-level adaptation, either for a fossil lepiodsaur or as part of an extant phylogenetic bracket (Witmer, 1995) to interpret other extinct animals with preserved sclerotic rings, such as dinosaurs (Rinehart et al., 2004; Schmitz, 2008). Even though the lepidosaur eyeball follows an organizational pattern consistent with light-level adaptation (Hall, 2005, 2008a), also seen in another group of extant diapsids, the avians (Hall, 2005, 2008b; Hall and Ross, 2007; Schmitz et al., 2007), the lepidosaur skull may simply not be sufficiently ossified to provide enough clues for reliable interpretation of visual adaptations from hard-tissue characteristics alone.

ACKNOWLEDGMENTS

The author thanks the American Museum of Natural History (New York, NY), the Field Museum of Natural History (Chicago, IL), the British National Museum of Natural History (London, UK), and the California Academy of Sciences (San Francisco, CA) for access to specimens. This work was part of a Ph.D. thesis, and here the author thanks the advisory committee, including Drs. Callum Ross, Matthew Carrano, Susan Evans, Catherine Forster, William Jungers, and Nathan Kley. In addition, the author thanks Drs. Christopher Heesy, Keith Metzger, Randall Nydam, Patrick O'Connor, Maureen O'Leary, F. James Rohlf, Karen Samonds, Lars Schmitz, Beth Townsend, Lawrence Witmer, and Myriam Zylstra for helpful comments. The author also thanks Drs. Christopher Heesy and Jason Kamilar for invaluable assistance in the phylogenetic analysis. The author thanks Dr. Randall Nydam for the photo in Fig. 2, Dr. Beth Townsend for constructing Figs. 1 and 2, and two anonymous reviewers for useful comments in preparing the final version of this manuscript.

LITERATURE CITED

Brooke MdL, Hanley S, Laughlin SB. 1999. The scaling of eye size and body mass in birds. Proc R Soc Lond B 266:405–412.

Carranza S, Arnold EN, Mateo JA, Geniez P. 2002. Relationships and evolution of the North African geckos, *Geckonia* and *Tarentola* (Reptilia: Gekkonidae), based on mitochondrial and nuclear DNA sequences. Mol Phylogenet Evol 23:244–256.

Cartmill M. 1970. The orbits of arboreal mammals: a reassessment of the arboreal theory of primate evolution. Unpublished Ph.D. dissertation, University of Chicago, Chicago, Illinois.

Chapple DG. 2003. Ecology, life-history, and behavior in the Australian scincid genus *Egernia*, with comments on the evolution of complex sociality in lizards. Herpetol Monogr 17:145–180.

Cogger HG. 1994. Reptiles and amphibians of Australia. Ithaca: Cornell University Press.

Cogger HG, Zweifel RG. 1992. Encyclopedia of reptiles and amphibians. New York: Academic Press.

Columbre AJ, Crelin ES. 1957. The role of the developing eye in the morphogenesis of the avian skull. Am J Phys Anthropol 16:25–37.

Donnellan SC, Hutchinson MN, Saint KM. 1999. Molecular evidence for the phylogeny of Australian gekkonid lizards. Biol J Linn Soc 67:97–118.

Endler JA. 1993. The color of light in forests and its implications. Ecol Monogr 63:1–27.

Fellers G, Drost CA. 1991. Ecology of the island night lizard, *Xantusia riversiana*, on Santa Barbara Island, California. Herpetol Monogr 5:28–78.

Felsenstein J. 1985. Phylogenies and the comparative method. Am Nat 125:1–15.

Fernandez MS, Archuby F, Talevi M, Ebner R. 2005. Ichthyosaurian eyes: paleobiological information content in the sclerotic ring of *Caypullisaurus* (Ichthyosauria, Ophthalmosauria). J Vert Paleontol 25:330–337.

Fitzgerald LA, Cook JA, Aquino AL. 1999. Molecular phylogenetics and conservation of *Tupinambis* (Sauria: Teiidae). Copeia 1999:894–905.

Franz-Odendaal TA. 2008. Scleral ossicles of teleostei: evolutionary and developmental trends. Anat Rec 291:161–168.

Franz-Odendaal TA, Hall BK. 2006. Skeletal elements within teleost eyes and a discussion of their homology. J Morphol 267:1326–1337.

Franz-Odendaal TA, Vickaryous MK. 2006. Skeletal elements in the vertebrate eye and adnexa: morphological and developmental perspectives. Dev Dyn 235:1244–1255.

Frost D, Janies D, Mouton PLFN, Titus T. 2001. A molecular perspective on the phylogeny of the girdled lizards (Cordylidae, Squamata). Am Mus Nov 3310:1–10.

Fu J. 1998. Toward the phylogeny of the family Lacertidae: implications from mitochondrial DNA 12S and 16S gene sequences (Reptilia: Squamata). Mol Phylogenet Evol 9:118–130.

Green SB, Salkind NJ, Akey Tm. 2000. Using SPSS for windows: analyzing and understanding data. New Jersey: Prentice Hall.

Greer AE 1989. The biology and evolution of australian lizards. Chipping Norton, NSW: Surrey Beatty and Sons.

Hair JF, Anderson RE, Tatham RL, Black WC. 1998. Multivariate data analysis. New Jersey: Prentice Hall.

Han D, Zhou K, Bauer AM. 2004. Phylogenetic relationships among gekkotan lizards inferred from C-*mos* nuclear DNA sequences and a new classification of the Gekkota. Biol J Linn Soc 83:353–368.

Hall MI. 2004. A new approach for inferring activity pattern in avians using the orbit and sclerotic ring. J Vert Paleontol 24(Supp 3):67A.

Hall MI. 2005. The roles of function and phylogeny in the morphology of the diapsid visual system. Unpublished Ph.D. dissertation, Stony Brook University, Stony Brook, New York.

Hall MI. 2008a. Comparative analysis of the size and shape of the lizard eye. Zoology 111:62–75.

Hall MI. 2008b. The anatomical relationships between the avian eye, orbit, and sclerotic ring: implications for inferring activity patterns in extinct birds. J Anat 212:781–794.

Hall MI, Heesy CP, Carrano MT. 2007. Inferring binocular visual field overlap in non-avian dinosaurs based on an extant avian scaling model. J Integr Comp Biol 46(Suppl 1):e204.

Hall MI, Ross CF. 2007. Eye shape and activity pattern in birds. J Zool 271:437–444.

Hanken J. 1983. Miniaturization and its effects on cranial morphology in plethodontid salamanders, genus *Thorius* (Amphibia, Plethodontidae). II. The fate of the brain and sense organs and their role in skull morphogenesis and evolution. J Morphol 177:255–268.

Hanken J, Thorgood P. 1993. Evolution and development of the vertebrate skull: the role of pattern formation. TREE 8:9–15.

Harvey PH, Pagel MD. 1991. The comparative method in evolutionary biology. Oxford: Oxford University Press.

Heesy CP, Ross CF. 2001. Evolution of activity patterns and chromatic vision in primates: morphometrics, genetics and cladistics. J Hum Evol 40:111–149.

Heesy CP, Ross CF. 2004. Mosaic evolution of activity pattern, diet, and color vision in haplorhine primates. In: CF Ross, Kay RF, editors. Anthropoid origins: new visions.New York: Kluwer Academic/Plenum Publishers. p 665–698.

Howland HC, Merola S, Basarab JR. 2004. The allometry and scaling of the size of vertebrate eyes. Vis Res 44:2043–2065.

Hughes A. 1977. The topography of vision in mammals of contrasting life style: comparative optics and retinal organisation. In: Crescitelli F, editor. The visual system in vertebrates. Berlin: Springer Verlag. p 613–756.

Humphries S, Ruxton GD. 2002. Why did some icthyosaurs have such large eyes? J Exp Biol 205:439–441

Kay RF, Cartmill M. 1977. Cranial morphology and adaptations of *Palaechthon nacimienti* and other Paromomyidae (Plesiadapoidea, Primates), with a description of a new genus and species. J Hum Evol 6:19–35.

Kay RF, Kirk EC. 2000. Osteological evidence for the evolution of activity pattern and visual acuity in primates. Am J Phys Anthropol 113:235–262.

Kiltie RA. 2000. Scaling of visual acuity with body size in mammals and birds. Funct Ecol 14:226–234.

Kirk EC. 2004. Comparative morphology of the eye in primates. Anat Rec A 281:1095–1103.

Kirk EC. 2006. Effects of activity pattern on eye size and orbital aperture size in primates. J Hum Evol 51:159–170.

Land MF, Nilsson D-E. 2002. Animal eyes. New York: Oxford University Press.

Lee MSY. 1998. Convergent evolution and character evolution in burrowing reptiles: toward a resolution of squamate relationships. Biol J Linnean Soc 65:369–453.

Lee MSY, Reeder TW, Slowinski JB, Lawson R. 2004. Resolving reptile relationships: molecular and morphological markers. In: Cracraft J, Donoghue MJ, editors. Assembling the tree of life. New York: Oxford University Press. p 451–467.

Macey JR, Schulte JA, II, Larson A, Tuniyev BS, Orlov N, Papenfuss TJ. 1999. Molecular phylogenetics, tRNA evolution, and historical biogeography in Anguid lizards and related taxonomic families. Mol Phylogenet Evol 12:250–272.

Maddison WP, Maddison DR. 2003. Mesquite: a modular system for evolutionary analysis. Version 1.05. Available at: http://mesquiteproject.org.

Martin GR. 1982. An owl's eye: schematic optics and visual performance in *Strix aluco*. J Comp Physiol 145:341–349.

Martin GR. 1985. Eye. In: King AS, McLelland J, editors. Form and function in birds, Vol. 3. New York: Academic Press. p 311–373.

Martin GR. 1990. Birds by night. San Diego: Academic Press.

Mattison C. 1989. Lizards of the world. New York: Facts on File, Inc.

Metzger KA, Herrel A. 2005. Correlations between lizard cranial shape and diet: a quantitative, phylogenetically informed analysis. Biol J Linn Soc 86:433–466.

Moss ML, Young RW. 1960. A functional approach to craniology. Am J Phys Anthropol 18:281–292.

Motani R, Rothschild BM, Wahl W, Jr. 1999. Large eyeballs in diving ichthyosaurs. Nature 402:747.

Nunn CL, Barton RA. 2001. Comparative methods for studying primate adaptation and allometry. Evol Anthropol 10:81–98.

Odierna G, Canapa A, Andreone F, Aprea G, Barucca M, Capriglione T, Olmo E. 2002. A phylogenetic analysis of Cordyliformes (Reptilia: Squamata): comparison of molecular and karyological data. Mol Phylogenet Evol 23:37–42.

Pianka ER, Vitt LJ. 2003. Lizards: windows to the evolution of diversity. Berkeley and Los Angeles: University of California Press.

Plotnick RE. 1989. Application of bootstrap methods to reduced major axis line fitting. Syst Zool 38:144–153.

Proctor NS, Lynch PJ. 1993. Manual of ornithology: avian structure and function. New Haven: Yale University Press.

Purvis A, Rambaut A. 1995. Comparative analysis by independent contrasts (CAIC): an Apple Macintosh application for analysing comparative data. Comput Appl Biosci 11:247–251.

Rayner JMV. 1985. Linear relations in biomechanics: the statistics of scaling functions. J Zool Lond 206:415–439.

Reeder TW, Cole CJ, Dessauer HC. 2002. Phylogenetic relationships of whiptail lizards of the genus *Cnemidophorus* (Squamata: Teiidae): a test of monophyly, reevaluation of karyotypic evolution, and review of hybrid origins. Am Mus Nov 3365:1–61.

Ricker WE. 1984. Computation and uses of central trend lines. Can J Zool 62:1897–1905.

Rinehart L, Lucas S, Heckert A, Hunt A. 2004. Vision characteristics of *Coelophysis bauri* based on sclerotic ring, orbit, and skull morphology. J Vert Paleo 24(Supp 3):104A.

Ritland S. 1982. The allometry of the vertebrate eye. Ph.D. thesis, University of Chicago, Chicago.

Röll B. 2001. Gecko vision—retinal organization, foveae, and implications for binocular vision. Vis Res 41:2043–2056.

Romer AS. 1956. Osteology of the reptiles. Chicago: University of Chicago Press.

Ross CF. 2000. Into the light: the origin of Anthropoidea. Annu Rev Anthropol 29:147–194.

Ross CF, Hall MI, Heesy CP. 2007. Were basal primates nocturnal? Evidence from eye size and shape. In: Ravosa M, Dagosto M, editors. Primate origins and adaptations. New York: Kluwer Academic/Plenum Publishers. p 257–277.

Rowe MP. 2000. Inferring the retinal anatomy and visual capacities of extinct vertebrates. Palaeontol Electron 3:43.

Schmitz L. 2008. Inference of diel activity pattern suggests complex temporal resource and habitat partitioning among *Mesozoic archosaurs*. J Vert Paleo 28(Suppl 3):137A.

Schmitz L, Motani R, Milner A. 2007. Diel activity pattern of Archaeopteryx. J Vert Paleo 27(Suppl 3):142A.

Schulte JA, II, Macey R, Larson A, Papenfuss TJ. 1998. Molecular tests of phylogenetic taxonomies: a general procedure and example using four subfamilies of the lizard family Iguanidae. Mol Phylogenet Evol 10:367–376.

Schulte JA, II, Valladares JP, Larson A. 2003. Phylogenetic relationships within Iguanidae inferred using molecular and morphological data and a phylogenetic taxonomy of Iguanian lizards. Herpetologica 59:399–419.

Schultz AH. 1940. The size of the orbit and of the eye in primates. Am J Phys Anthropol 26:389–408.

Smith HM. 1946. Handbook of lizards: lizards of the United States and of Canada. Ithaca: Cornell University Press.

Sokal RR, Rohlf FJ. 1995. Biometry, 3rd ed. New York: W.H. Freeman and Co.

Taylor WOG. 1939. Effect of enucleation of one eye in childhood on the subsequent development of the face. Trans Ophthalmol Soc UK 59:361–371.

Thorogood P. 1988. The developmental specification of the vertebrate skull. Development 103(Suppl):141–153.

Tonneyckmuller I. 1974. Growth of eyes and orbits in chicken embryo. VIII. Development of skull in embryos of 12–17 days with artificially induced bilatera micropthalmia. Acta Morphol Neerl Scand 12:145–158.

Townsend T, Larson A. 2002. Molecular phylogenetics and mitochondrial genomic evolution in the Chamaeleonidae (Reptilia, Squamata). Mol Phylogenet Evol 23:22–36.

Underwood G. 1970.The eye. In: Gans C, Parsons TS, editors. Biology of the reptilia, Vol. 2: Morphology B. London:Academic Press. p 1–97.

Vanlimborgh J, Tonneyckmuller I. 1976. Experimental studies on relationships between eye growth and skull growth. Ophthalmologica 173:317–325.

Vicario S, Caccone A, Gauthier J. 2003. Xantusiid "night" lizards: a puzzling phylogenetic problem revisited using likelihood-based Bayesian methods on mtDNA sequences. Mol Phylogenet Evol 26:243–261.

Walls GL. 1942. The vertebrate eye and its adaptive radiation. New York: Hafner.

Werner YL. 1969. Eye size in geckos of various ecological types. Israel J 2001 18:291–316.

Werner YL, Seifan T. 2006. Eye size in geckos: asymmetry, allometry, sexual dimorphism, and behavioral correlates. J Morph 267: 1486–1500.

Whiting AS, Bauer AM, Sites JW. 2003. Phylogenetic relationships and limb loss in sub-Saharan African scincine lizards (Squamata: Scincidae). Mol Phylogenet Evol 29:582–598.

Wiens JJ, Hollingsworth BD. 2000. War of the iguanas: conflicting molecular and morphological phylogenies and long-branch attraction in Iguanid lizards. Syst Biol 49:143–159.

Witmer LM. 1995. The extant phylogenetic bracket and the importance of reconstructing soft tissues in fossils. In: Thomason JJ, editor. Functional morphology in vertebrate paleontology. Cambridge: Cambridge University Press. p 19–33.